Molecular Dynamics Simulations of Comb-Branched Poly(epoxide ether)-Based Polymer Electrolytes

Oleg Borodin* and Grant D. Smith

Department of Materials Science & Engineering, 122 S. Central Campus Dr, Rm 304, University of Utah, Salt Lake City, Utah 84112-0560

Received September 13, 2006; Revised Manuscript Received December 20, 2006

ABSTRACT: Molecular dynamics (MD) simulations using many-body polarizable force field were performed on comb-branched poly(epoxide ether) (PEPE) polymer electrolytes doped with lithium bistrifluoromethanesulfonamide (LiTFSI) salt as a function of temperatures from 333 to 423 K at ether oxygen (EO) to lithium ratio of 20. MD simulations predicted electrolyte conductivity in good agreement with experiments. The fraction of solvent-separated ions and lithium cation environment for PEPE/LiTFSI were similar to those found for the linear poly(ethylene oxide) (PEO)/LiTFSI electrolyte. The Li^+ cations had the highest probability to be coordinated by EOs near the PEPE polymer backbone and the lowest probability being coordinated by EO's at the end of side chains. Segmental dynamics of the backbone was slower by 2 orders of magnitude compared to the dynamics of side-chain ends. The Li^+ self-diffusion coefficient was approximately an order of magnitude lower than the $TFSI^-$ anion self-diffusion coefficient. Visualization of the lithium motion revealed that the most mobile Li^+ cations moved by hopping from a side chain to another without being complexed by the backbone. The influence of the backbone−Li^+ interactions and the backbone stiffness on ion transport was investigated in MD simulations performed on the PEPE/LiTFSI-like electrolytes with the same PEPE architecture but a very stiff backbone that does not complex lithium cations. The ion transport in these model electrolytes was compared to that of the original PEPE/LiTFSI electrolyte.

I. Introduction

Solid polymer electrolytes (SPEs) and gel electrolytes are being widely investigated for use in various types of lithium batteries.[1] SPEs combine ease of fabrication, good electrochemical stability, low flammability, and toxicity with the ability to form good interfacial contact with electrodes during charge−discharge cycles and eliminate a need for a separator. Despite these advantages over liquid electrolytes, current SPEs exhibit low ambient temperature conductivity, low lithium transference numbers, and high interfacial impedance, preventing them from being used in batteries for consumer electronics and automotive applications.[1,2] Plasticizing SPEs with traditional carbonate solvents, forming gel electrolytes, has resulted in improved ion transport but poor mechanical properties and high solvent volatility.[1]

Comb-branched polymer architectures are convenient for optimization of the SPE properties because they prevent polymer crystallization if relatively short side chains are used,[2,3] allow separate optimization of the backbone properties from those of side chains with a wide variety of chemistries available, and offer a potential for an anion attachment to side chains in order to achieve single-ion conducting behavior.[4−8] Experimental investigations of comb-branched polymer architectures concentrated on PEO-grafted polymethacrylates,[9] polyphosphazene with oligoether side chains,[10−13] and other comb-branched polymers with oligoether side chains[2,3,14] with polyepoxide, polyacrylate, or polyvinylbenzyl backbones.[15−17] Importantly, comb-branched structures allow optimization of the charge-transfer process that often leads to reduced interfacial impedance compared to linear PEO-based SPEs.[9,18,19]

Molecular dynamics (MD) simulation studies overwhelmingly concentrated on understanding of the structure−transport relationship and the mechanisms of Li^+ transport in linear polyethers,[20−35] partly because this task was challenging in itself due to complicated transport mechanism and long characteristic time scales associated with a lithium motion in a polymer. Only recently, long (∼50 ns) simulations with accurate force fields allowed detailed quantification of the mechanisms contributing to the Li^+ transport in linear PEO-based polymer electrolytes.[36] Simulations of the lithium salts in comb-branched polymer structures are limited to a few publications[37,38] and were focused on extracting structural information from relatively short (<1 ns) trajectories. Balbuena's group[38] performed subnanosecond simulations of polyphosphazene with oligoether side chains that qualitatively predicted the Li^+ preference to be complexed by the backbone. However, the electrostatic interactions had to be decreased by a factor of 3 in her simulations to speed up Li^+ dynamics because Li^+ was not moving during subnanosecond simulations at 393 K when the original force field was used.[37] Her simulations were too short to discern details of the Li^+ transport mechanism despite facilitated ion dynamics achieved by reducing all electrostatic interactions. Our simulations presented below indicate that the Li^+ residence time near side chains is 33 ns at 393 K, thus requiring simulations for tens of nanoseconds in order to observe Li^+ exchanges between side chains at this temperature and to extract a reliable Li^+ self-diffusion coefficient. Aabloo's group[39] has looked at local mobility of the ether oxygen atoms for comb-branched polymers without lithium salt as it is relevant to the Li^+ transport in such polymer hosts.

It is the goal of the present simulation study to test the ability of the recently derived quantum-chemistry-based force field[40,41] to be able to accurately predict ion transport in comb-branched poly(epoxide ether) (PEPE)-based polymer electrolytes and to perform simulations long enough to be able to extract mechanisms of the Li^+ transport in the PEPE comb-branched polymer host. The Li^+ environment and transport mechanisms are compared with those from our previous simulations of the linear PEO/LiTFSI.[36] Influence of the Li^+−backbone interactions and the backbone stiffness on Li^+ transport will be studied in

10.1021/ma062128s CCC: $37.00 © 2007 American Chemical Society
Published on Web 01/24/2007

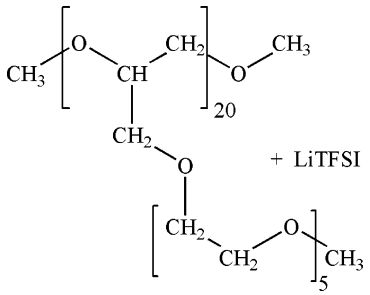

Figure 1. Chemical structure of the simulated isotactic $PEPE_5$ comb-branched polymer doped with LiTFSI.

additional MD simulations performed on the PEPE/LiTFSI-like electrolyte with the same PEPE architecture but a very stiff backbone that also does not complex lithium cations.

II. Molecular Dynamics Simulation Methodology

MD simulations were performed on comb-branched poly(epoxide ether)s (PEPE) with the structure shown in Figure 1. The PEPE host was doped with LiTFSI corresponding to ether oxygen (EO):Li = 20 salt concentration. Simulations were performed at temperatures from 333 to 423 K, as shown in Table 1. A version of the MD simulation package Lucretius[42] that includes many-body polarization was used for all MD simulations. The many-body force field previously developed[40,41] was used. The three-dimensional, periodic cubic simulation cell consisted of 21 LiTFSI + 3 $PEPE_5$ chains with 141 EO groups per $PEPE_5$ chain. All electrolytes were created in the gas phase corresponding to a cell (linear) dimension of ~180 Å. The cell was shrunk to the size corresponding to a density that yielded an average pressure of 1 atm over 1 ns at 423 K simulations using a Brownian dynamics. Simulations were first performed at 423 K. After approximately 40−60% of the trajectory at 423 K was generated, the temperature was decreased to 393 K. The same procedure was repeated at 363 and 333 K. Table 1 summarizes the length of the production and equilibration runs performed using NVT and NPT ensembles, respectively.

A Nośe-Hoover thermostat and a barostat were used to control the temperature and pressure with the associated frequencies 10^{-2} and 10^{-3} fs^{-1}.[43] Bond lengths were constrained using the Shake algorithm.[43] The Ewald summation method[43] was used for treatment of long-range electrostatic forces between partial charges and between partial charges and induced dipoles for the many-body polarizable potential. The Ewald convergence parameter α was set to 8 Å. The number of reciprocal space vectors was set to 6.[3] A tapering function was used for scaling the induced dipole−induced dipole interactions to zero at the cutoff of 10 Å, with scaling starting at 9 Å. A multiple time step reversible reference system propagator algorithm[44] was employed, with a time step of 0.5 fs for bonding, bending, and torsional motions, a 1.5 fs time step for nonbonded interactions within a 6.5 Å sphere, and a 3.0 fs time step for nonbonded interactions between 6.5 and 10.0 Å and the reciprocal space part of the Ewald summation. Coordinates were stored every 1 ps.

We also performed MD simulations of the $PEPE_5$/LiTFSI electrolyte utilizing a modified Li···C* repulsion parameters of 958610 exp(−3.8*r*) (kcal/mol) compared to the original force field values of 95861 exp(−4.346*r*) (kcal/mol), where C* is the carbon atom connecting a side chain to the backbone and *r* is the Li···C distance in angstroms. The increased Li···C* repulsion parameters prevent Li^+ cations from being complexed by the backbone ether oxygen atoms. The influence of the backbone stiffness was investigated by increasing the barriers for the conformational transitions of the −O−C−C−O− and −C−C−O−C− dihedrals by 5 kcal/mol. The length of these simulations is also summarized in Table 1.

III. Electrolyte Density and Li^+ Environment

The densities of the $PEPE_5$/LiTFSI electrolyte predicted by MD simulations are shown in Table 1. Comparing the $PEPE_5$/LiTFSI densities with those for the linear PEO(M_w = 2380)/LiTFSI electrolyte at the same salt concentration[36] indicates that the densities of the linear and comb-branched SPEs differ by less than 1%. The similarity of densities indicates that the free volume is similar in these two electrolytes.

We find that the Li^+ local environment in the $PEPE_5$/LiTFSI electrolyte is also almost identical to that observed in previous simulations[36] of PEO(M_w = 2380)/LiTFSI SPEs. Specifically, the Li^+ cations have on average 4.3 ± 0.2 ether oxygen (EO) atoms within 2.8 Å. When the radius of the Li^+ coordination shell is extended to 4 Å to include loosely coordinated EO atoms, each Li^+ is coordinated by about six EO atoms in accord to coordinations found in $glyme_2$/LiTFSI crystal structures.[45] A more detailed analysis of the Li^+ complexation that is done separately for EO atoms depending on their position in the chain is shown in Figure 2. We enumerated EO atoms based on their proximity to the backbone. The EO belonging to the $PEPE_5$ backbone is labeled as EO_0, the first EO in the side chain adjacent to the backbone is denoted as EO_1, etc. The last EO located at the side-chain end is labeled as EO_6. We observe that the Li^+ cations have the highest probability to be coordinated by EOs from the comb-branch polymer backbone and the one adjacent to it denoted as EO_0 and EO_1. The lowest probability for the Li^+ coordination is found to the EOs from side-chain ends (EO_6). These results are in accord with our previous reports,[46] indicating that in linear polyethers Li^+ cations have the highest probability to be located in the middle of a chain and the lowest probability to be coordinated by chain ends. Interestingly, quantum chemistry calculations,[38] MD simulations,[38] and experiments[11] of bis(methoxyethoxyethoxy)phosphazene (MEEP) also showed the Li^+ preference to be coordinated by backbone atoms: the nitrogen in the case of MEEP.

The fraction of Li^+ cations separated from the $TFSI^-$ anions by oligoether chains, denoted as α_s, is summarized in Table 1. We observe a high degree of the cation−anion separation (dissociation), 79−95%, and essentially no difference between results for $PEPE_5$/LiTFSI and PEO/LiTFSI.[33,36] The degree of dissociation increases with decreasing temperature and is higher than the values observed at similar salt concentration for other anions in previous simulation of Li-salt doped oligoether electrolytes.[31,36,46−49]

IV. Transport Properties

A. Ion and Solvent Self-Diffusion Coefficients. The self-diffusion coefficient D_i for species *i* was calculated using Einstein relation[43] for the $TFSI^-$ anion and Li^+ cation at 423 K.

$$D_i = \lim_{t\to\infty} D_i^{\mathrm{app}}(t) = \lim_{t\to\infty} \frac{\langle \mathrm{MSD}_i(t)\rangle}{6t} \qquad (1)$$

where $\mathrm{MSD}_i(t)$ is mean-square displacement of a molecule center-of-mass during time *t*, $\langle\ \rangle$ denotes an ensemble average, and $D_i^{\mathrm{app}}(t)$ is the time-dependent apparent diffusion coefficient. The Li^+ and $TFSI^-$ $\mathrm{MSD}_i(t)$ are shown in the Supporting Information. At 423 K the Li^+ motion is subdiffusive, i.e., $\mathrm{MSD}_i(t) \sim t^{\gamma}$ with $\gamma < 1$, on a time scale of tens of nanoseconds and

Table 1. Length of MD Simulations, Electrolyte Density, Fractions of Free Ions ($r(Li^+-N) > 5$ Å), and Degree of Ion Uncorrelated Motion (α_d)

temp (K)	equilibration run length (ns)	production run length (ns)	density (kg m^{-3})	fraction of free ions (α_s)	α_d
		original force field			
423	3	38	1144	0.80	0.8_3
393	2	24	1170	0.88	0.8_6
363	2	30	1198	0.89	0.9_0
333	2	8	1227	0.94	0.9_5
		increased Li^+−(polymer backbone repulsion)			
393	1	6	1170	0.81	
		stiffened $PEPE_5$ backbone with the increased Li^+−(polymer backbone) repulsion			
423	1	5	1144	0.67	
393	1	29	1170	0.86	0.8_0
363	1	4.5	1198	0.91	

is similar to the previously shown data for PEO/LiTFSI.[36] In contrast, the $TFSI^-$ anion diffuses relatively rapidly and becomes diffusive on the time scale of a few nanoseconds in accord to previous results for PEO/LiTFSI.[36] As temperature decreases, longer simulations are required in order to reach the diffusive regime. Such simulations are very expensive using the many-body polarizable potentials we employed, thus posing significant difficulties for obtaining the ion self-diffusion coefficient at low temperatures. In order to estimate the ion self-diffusion coefficient as accurately as possible at low temperatures, we followed our previous work[36,50] and assumed that $MSD_i(t)$ at different temperatures can be superimposed by scaling the time axis. The self-diffusion coefficients of all ions are determined as

$$D_i(T) = D_i(423\ \mathrm{K})/a_i(T) \tag{2}$$

where $D_i(423\ \mathrm{K})$ was obtained utilizing eq 1 at 423 K and $a_i(T)$ is the temperature-dependent time-shift factor obtained by superimposing $MSD_i(t)$. Figure 3 shows a comparison of the Li^+ and $TFSI^-$ self-diffusion coefficients for $PEPE_5$/LiTFSI with the results of previous simulations[36] for PEO(M_w = 2380)/LiTFSI at the same salt concentration. The $TFSI^-$ anion self-diffusion coefficients are very similar for the linear and comb-branched polymer electrolyte, while the Li^+ self-diffusion coefficient is a factor of 2.5−5 slower for $PEPE_5$/LiTFSI compared to PEO/LiTFSI. We attribute the lower Li^+ self-diffusion coefficient in the comb-branched electrolyte to the slow mobility of Li^+ cations coordinated with the slowly relaxing backbone, as will be demonstrated below.

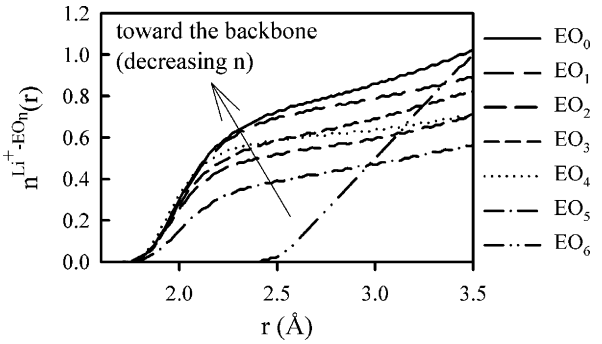

Figure 2. Running coordination number of EO within radius r of a Li^+ for $PEPE_5$/LiTFSI at 393 K. Plots for the EO groups with various proximity to the $PEPE_5$ backbone are shown. The EO_0 belongs to the backbone and EO_n ($n > 0$) belong to the $PEPE_5$ side chains, where n is the repeat units number from the backbone.

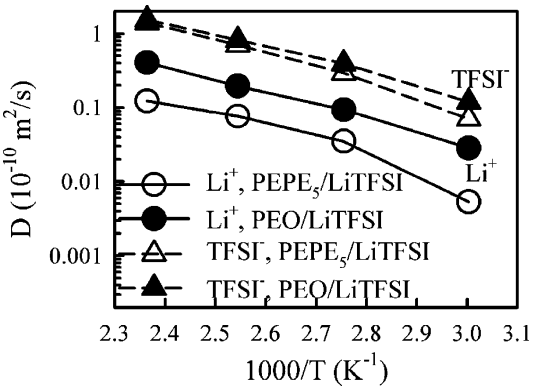

Figure 3. Ion self-diffusion coefficients for $PEPE_5$/LiTFSI and linear PEO/LiTFSI from simulations[36] and experiments.[3,14,57] The linear PEO M_w = 2380 for MD and 2480 for experimental samples.[57]

The apparent lithium transference number t_+^{app} was calculated as

$$t_+^{app} = \frac{D_{Li^+}}{D_{Li^+} + D_{TFSI^-}} \tag{3}$$

t_+^{app} values of 0.07−0.1 were obtained for $PEPE_5$/LiTFSI, consistent with the experimentally measured[51] apparent lithium transference values 0.05−0.08 for the similar polyether-based hyperbranched network SPEs doped with LiTFSI at EO:Li = 17 salt concentration and are indicative that, unfortunately, a dominant fraction of the charge transport is due to $TFSI^-$ anion motion in comb-branched electrolytes. The $PEPE_5$ self-diffusion coefficient of $PEPE_5$ polymer host is estimated to be more than an order of magnitude lower than that for the Li^+, indicating that the $PEPE_5$ chains are essentially immobile in comparison with the Li^+ cations and the contribution from the Li^+ motion together with the $PEPE_5$ chain center of mass to the Li^+ transport is negligible; thus, we expect the Li^+ self-diffusion coefficient from our simulations to be similar to the one for high molecular weight polymeric electrolytes.

B. Correlation of Ion Motion and Electrolyte Ionic Conductivity. Ionic conductivity is the long time limit of apparent conductivity $\lambda^{app}(t)$ and is calculated using the Einstein relation[43]

$$\lambda = \lim_{t\to\infty} \lambda^{app}(t) = \lim_{t\to\infty} \frac{e^2}{6tVk_BT} \sum_{i,j}^{N} z_i z_j \langle ([\mathbf{R}_i(t) - \mathbf{R}_i(0)])([\mathbf{R}_j(t) - \mathbf{R}_j(0)])\rangle \tag{4}$$

where e is the electron charge, V is the volume of the simulation box, k_B is Boltzmann's constant, T is the temperature, t is time, z_i and z_j are the charges over ions i and j in electrons, $\mathbf{R}_i(t)$ is the displacement of the ion i during time t, the summation is performed over all ions, $\langle\ \rangle$ denotes the ensemble average, and N is the total number of ions in the simulation cell. Determining the long-time limit of $\lambda^{app}(t)$ using eq 4 is problematic even at high temperatures where the diffusion coefficients can be

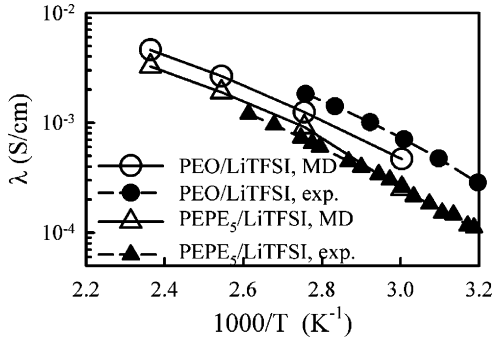

Figure 4. Ionic conductivity for $PEPE_5$/LiTFSI and PEO/LiTFSI from simulations[36] and experiments.[3,14,57] The linear PEO $M_w = 2380$ for MD and 2480 for experimental samples.[57]

accurately determined because $\lambda^{app}(t)$ has poorer statistics and a higher uncertainty compared to MSD(t).

Conductivity can be decomposed into an "ideal" conductivity that would be realized if ion motion were uncorrelated, denoted $\lambda_{uncorr}(t)$, and the degree to which ion motion is in fact uncorrelated, or α_d. The degree of uncorrelated ion motion is given as the ratio of the collective (total) charge transport (λ) to the charge transport due to self-diffusion only (λ_{uncorr})

$$\lambda^{app}_{uncorr} = \lim_{t\to\infty} \lambda^{app}_{uncorr}(t) = \lim_{t\to\infty} \frac{e^2}{6tVk_BT} \sum_i^n z_i^2 \langle [\mathbf{R}_i(t) - \mathbf{R}_i(0)]^2 \rangle = \frac{e^2}{Vk_BT} (n_{Li^+} D^{app}_{Li^+} + n_{TFSI^-} D^{app}_{TFSI^-}) \quad (5)$$

$$\alpha_d = \frac{\lambda}{\lambda_{uncorr}} = \lim_{t\to\infty} \alpha_d(t) = \lim_{t\to\infty} \frac{\lambda^{app}(t)}{\lambda^{app}_{uncorr}(t)} \quad (6)$$

Here n_i is the number of atoms of type i = (Li^+ or $TFSI^-$), $n = n_{Li^+} + n_{TFSI^-}$. The degree of ion uncorrelated motion $\alpha_d = 1$ corresponds to completely uncorrelated ion motion, while $\alpha_d = 0$ if all of the cations only move together with anions.

The $\alpha_d(t)$ were calculated using eq 6 and are shown in Table 1 as the averaged values for the time scale where we feel that adequate statistics is present for accurate determination of $\alpha_d(t)$, which is typically up to a few nanoseconds. We find that the length of the simulation run needs to be at least one but preferably 2 orders of magnitude longer than the time where a reliable estimate of the $\alpha_d(t)$ and λ are possible in accord with conclusions of the study investigating accuracy viscosity predictions as a function of the length of the simulation trajectory.[52] The α_d values are similar to the α_s (dissociated ion pairs from the structural analysis) indicative of good correlation between the fraction of free (uncomplexed by a counterion) ions and uncorrelated ion motion in the $PEPE_5$/LiTFSI electrolyte at EO: Li = 20 salt concentration. Next, we assumed that the α_d values from the nanosecond regime are similar to those at long times. This assumption allows us to estimate electrolyte conductivity using α_d and ion self-diffusion coefficients from eqs 5 and 6. Predicted conductivity is shown in Figure 4 along with data for linear PEO/LiTFSI from MD simulations and experiments.[3,53] MD simulation predictions of $PEPE_5$/LiTFSI are in good agreement with experimentally measured values in Kerr's group[3] for the higher molecular weight samples. As Li^+ motion together with a polymer host gives a negligible contribution to conductivity in our simulations of $PEPE_5$/LiTFSI and the chain end contribution to polymer local relaxation is also negligible for the simulated molecular weight, we expect very little changes

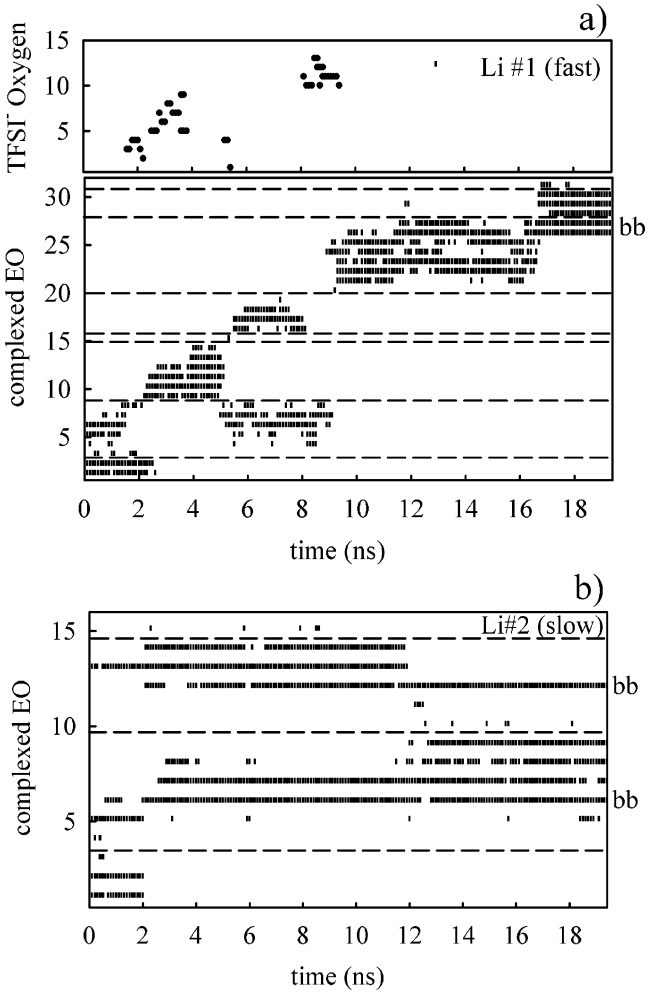

Figure 5. Plots of evolution of the Li^+ local environment with time for 2 Li^+ cations. Ether oxygen (and $TFSI^-$ oxygens) atoms complexed at each time interval of 100 ps for longer than 50 ps with a given Li^+ are marked with the filled symbol. Dashed lines separate ether oxygen belonging to the same side chain.

of the $PEPE_5$/LiTFSI conductivity with the increase of the polymer molecular beyond the simulated value, in agreement with experimental evidence for similar molecular weight linear polymer electrolytes.[53] Thus, the comparison between MD predictions and experiments is meaningful. Conductivity of $PEPE_5$/LiTFSI is slightly lower than conductivity of low molecular weight PEO-doped LiTFSI as a result of a lower cation diffusion shown in Figure 3.

V. Lithium Transport Mechanism

MD simulations present a unique opportunity for detailed analysis of the Li^+ transport mechanism. We begin by investigation of the changes in Li^+ coordination as a function of time for each Li^+. Changes in the Li^+ coordination are conveniently monitored utilizing the coordination plots shown in Figure 5. Here we follow the technique introduced by Müller-Plathe et al.;[20] specifically, all EO that are complexed by a Li^+ cation ($r(Li^+-O) < 2.8$ Å) are numbered consecutively from one end of a $PEPE_5$ chain to the other. If at any given time a Li^+ is coordinated by a specific EO, this EO is marked as a complexing EO for that cation and is shown in the plot as a filled symbol. In order to improve clarity of the plot and remove EO that participate in complexation for a very brief period of time, we show in Figure 5 only EO involved in complexing a Li^+ for at least 50 ps out of each 100 ps interval. The EO groups belonging

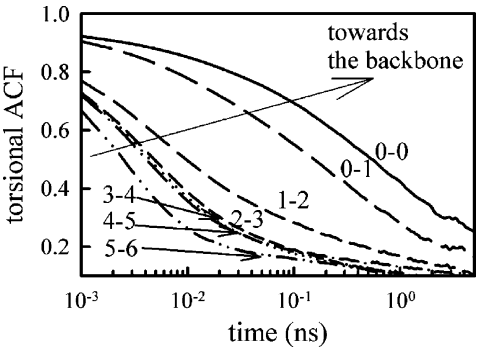

Figure 6. $-O_n-C-C-O_m-$ torsional ACF for $PEPE_5$ comb-branched polymer doped with LiTFSI salt (EO:Li = 20) at 393 K, where *n* and *m* denote proximity of the oxygen atom to the backbone with O_0 being the oxygen at the backbone and O_6 being the oxygen atom at the side chain end.

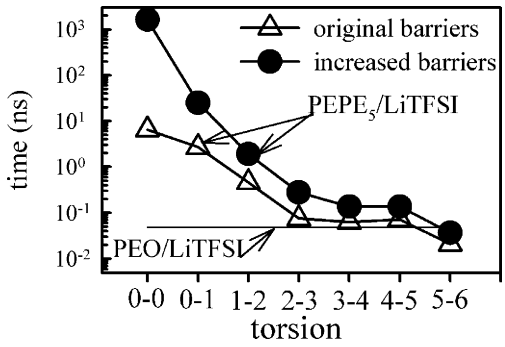

Figure 7. $-O_n-C-C-O_m-$ torsional autocorrelation time (for $P(t) = 0.2$)) for $PEPE_5$/LiTFSI and PEO(M_w = 2380), EO:Li = 20 at 393 K.

to the same side chain are marked by dashed lines. The EO groups belonging to the $PEPE_5$ backbone are marked on the left side of Figure 5. The oxygen atoms from $TFSI^-$ anions involved in complexing Li^+ are marked analogously to the complexed EO and are shown in Figure 5.

Figure 5 shows the evolution of a Li^+ coordination shell over time for two lithium cations that have quite different local mobility. The Li^+ cation examined in Figure 5a changes side chains multiple times during a part of the simulation, while the Li^+ shown in Figure 5b does not significantly change its coordination over time. Contrasting Figure 5a with 5b highlights significant heterogeneity of Li^+ motion on the scale of our simulations (~20 ns) at 393 K as some Li^+ undergo multiple changes of its coordination, whereas others (Figure 5b) basically do not change their coordination on the scale of 20 ns. We observe that the fast Li^+ (Figure 5a) displacement is ~5 times larger than that for the Li^+ shown in Figure 5b after 20 ns. We notice that the common feature of the low mobility lithiums is their complexation with the $PEPE_5$ backbone, while fast lithiums typically hop from a one side chain to another without being complexed by the $PEPE_5$ backbone. In order to understand the origin of such behavior, we characterized the conformation relaxation of the $PEPE_5$ comb-branched polymers as a function of proximity to the backbone via calculation of the $-O-C-C-O-$ torsional autocorrelation function (ACF) given by

$$P_i(t) = \frac{\langle \cos(\phi_{n-m}(t)) \cos(\phi_{n-m}(0)) \rangle - \langle \cos(\phi_{n-m}(0)) \rangle^2}{\langle \cos^2(\phi_{n-m}(0)) \rangle - \langle \cos(\phi_{n-m}(0)) \rangle^2} \quad (7)$$

where $\phi_{n-m}(t)$ is the $-O_n-C-C-O_m-$ dihedral angle, the subscripts *n* and *m* indicate dihedral number that is a function of its proximity to the $PEPE_5$ backbone, *t* is time, and the brackets denote an ensemble average over all dihedrals of type *i*. The $-O_n-C-C-O_m-$ torsional angles correspond to pairs of EO atoms (*n*, *m*) from Figure 2. The torsional ACF functions are shown in Figure 6. The decay of the torsional ACFs is depends strongly on the position in $PEPE_5$ chain. We have chosen a time where a torsional ACF reaches 0.2 as a characteristic relaxation time of the dihedral and plotted it in Figure 7. The $-O_n-C-C-O_m-$ dihedral autocorrelation time is the longest for the backbone dihedrals ($O_0-C-C-O_0$ or 0−0). It is more than 2 orders of magnitude longer than the relaxation time for the dihedrals in the middle of side chains and the average value for the $-O-C-C-O-$ relaxation in a linear PEO/LiTFSI electrolyte at the same temperature and salt concentration. The torsional autocorrelation times for the $-O_0-C-C-O_1-$ and $-O_1-C-C-O_2-$ dihedrals are also 1−2 orders of magnitude longer compared to the relaxation times for the dihedrals in PEO/LiTFSI, while the relaxation times for the dihedrals from $O_2-C-C-O_3$ to $O_4-C-C-O_5$ are very similar to those for the $-O-C-C-O-$ dihedrals in PEO/LiTFSI. The $O_5-C-C-O_6$ dihedral at the chain end shows the fastest relaxation as expected. We note that because of low lithium salt concentration EO:Li = 20 the majority of dihedrals are not complexed by Li^+ cations, indicating that the relaxation times shown in Figure 7 are dominated by the relaxation of dihedrals not complexed by Li^+ cations.

The correlations of ion dynamics with the glass transition temperature is widely known from experiments and is indicative of the coupling between ion transport and polymer relaxation.[2] MD simulations have also shown that the slowing down of conformational relaxation directly translates into slowing down of the Li^+ and $TFSI^-$ dynamics.[54] Thus, the slower by orders of magnitude relaxation of dihedrals near the $PEPE_5$ backbone is expected to result in a significant slowing down of the Li^+ dynamics for the cations that are complexed by the backbone groups. Two strategies for improving ion transport could be envisioned: the first one is to increase dynamics of the dihedrals near a backbone as realized in MEEP comb-branched polymers[10−13] and siloxanes with oligoether side chains.[55,56] The second strategy is to prevent Li^+ cations from being complexed by the slow-moving backbone. The drawback of the first strategy is the degradation of the polymer mechanical properties, while the second strategy results in losing some solvating groups.

VI. Influence of the Li^+−Backbone Interactions and Backbone Stiffness on Ion Transport

Additional MD simulations were performed at 393 K with the increased repulsive interactions between the Li^+ and backbone carbon atoms as described in the MD Methodology section. The resulting running coordination numbers of EOs near a Li^+ are shown in Figure 8. No Li^+ are coordinated by backbone atoms as expected due to increased Li^+−backbone carbon repulsion. The fraction of the Li^+ coordinating EO_1 is significantly reduced compared to results of the simulations utilizing the original force field and shown in Figure 2. The Li^+ self-diffusion coefficient for the $PEPE_5$/LiTFSI electrolyte with the repulsive Li^+−backbone interactions is ~30% higher than the Li^+ diffusion for the $PEPE_5$/LiTFSI simulated with the original force field. It is a modest improvement but could be easily achieved by incorporation less polarizable or less polar groups in the comb-branched polymer architecture.

As efficient Li^+ transport in $PEPE_5$/LiTFSI does not involve the comb-branched polymer backbone, one envisions that it is possible to improve mechanical properties of the SPE by using

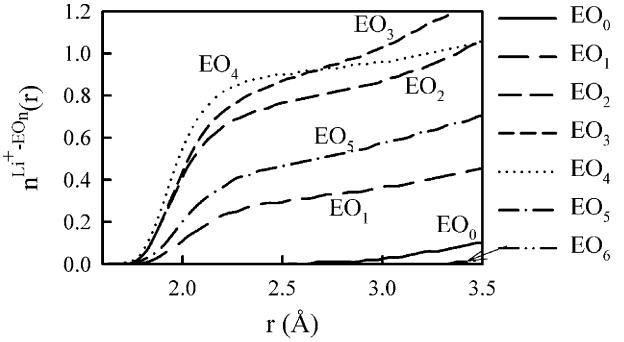

Figure 8. Running coordination number of EO within radius r of a Li^+ for $PEPE_5$/LiTFSI at 393 K from simulations with the increased Li^+−backbone repulsion. Plots for the EO groups with various proximity to the $PEPE_5$ backbone are shown.

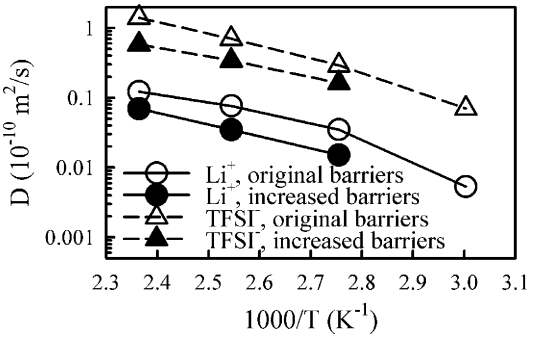

Figure 9. Ion self-diffusion coefficients for $PEPE_5$/LiTFSI for simulations with original backbone barriers and backbone barriers increased by 5 kcal/mol.

a stiff backbone that does not solvate (coordinate) Li^+ cations without significant degradation of the charge transport. To investigate this supposition, additional MD simulations with a very stiff backbone and the increased Li^+−backbone repulsion were performed. The backbone was stiffened by increasing barriers for the backbone C−O−C−C and O−C−C−O dihedrals by 5 kcal/mol. The Li^+ complexation by EO groups was similar to that shown in Figure 7. The characteristic relaxation times for the O−C−C−O dihedrals are shown in Figure 8. Increasing backbone barriers slows down backbone relaxation by more than 2 orders of magnitude, while the side-chain dihedrals slow down only by a factor of 2−4 compared to the original $PEPE_5$/LiTFSI electrolyte. The ion self-diffusion coefficients for electrolytes the stiff $PEPE_5$ polymer host and original one are shown in Figure 9. In the stiff $PEPE_5$/LiTFSI electrolyte both Li^+ and $TFSI^-$ ions move a factor of 2 ± 0.3 slower compared to the original $PEPE_5$/LiTFSI. Thus, slowing down of the backbone dynamics by 2 orders of magnitude leads to only a modest slowing down of ion dynamics. These results are in qualitative agreement of the experimental study of the influence of the backbone properties on conductivity of comb-branched polymers with oligoether side chains done by Kerr's group.[14]

VII. Conclusions

MD simulations utilizing recently developed many-body polarizable force fields accurately predicted conductivity of the $PEPE_5$/LiTFSI comb-branched polymer electrolyte as a function of temperature at EO:Li = 20 salt concentration. As found for linear PEO/LiTFSI electrolytes at EO:Li = 20, the fraction of the solvent separated ion pairs was quite high (0.8−0.95), suggesting that most of the charge transport is due to ions uncomplexed by a counterions. The Li^+ self-diffusion coefficient was found to be roughly an order of magnitude lower than the $TFSI^-$ anion self-diffusion coefficient, indicating that most of the charge transport is due to anion.

The conformational relaxation of the comb-branched polymer backbone was up to 2 orders of magnitude slower compared to the relaxation of the middle of side chains, which was in turn quite similar to the relaxation of in the linear PEO-doped LiTFSI. Because of the slow backbone relaxation, the Li^+ cations complexed by the PEPE backbone exhibited slower dynamics compared to other Li^+ cations that moved from the PEPE side chain to a side chain without being complexed by the backbone groups. Forcing Li^+ cations not to be solvated (coordinated) by the backbone resulted in an improvement of the Li^+ transport by 30%.

An additional electrolyte that has a stiff backbone with barriers for the backbone group conformation transitions raised by 5 kcal/mol and Li^+ cations not solvated (complexed) by the backbone was investigated. In this electrolyte ions move only a factor of 2 ± 0.3 slower compared to the original $PEPE_5$/LiTFSI electrolyte despite slower by 2 orders of magnitude backbone dynamics in the former. Thus, only a modest slowing down of ion dynamics is observed with a dramatic stiffening of a polymer chain, suggesting a possibility for a partial decoupling of electrolyte mechanical properties and ion transport. Such electrolytes might present a compromise for improving electrolyte mechanical properties accompanied by a modest loss of conductivity.

Acknowledgment. The authors are grateful to John Kerr (LBNL) for very stimulating discussions, providing experimental data and ideas. The financial support of this work by the Assistant Secretary for Energy Efficiency and Renewable Energy, Office of FreedomCAR and Vehicle Technologies of the U.S. Department of Energy, under Contract No. DE-AC02-05CH11231 on PO No. 6515401 is acknowledged.

Supporting Information Available: Li^+ cation and $TFSI^-$ anion mean-squared displacements as a function of time and scaled time. This material is available free of charge via the Internet at http://pubs.acs.org.

References and Notes

(1) Tarascon, J. M.; Armand, M. *Nature (London)* **2001**, *414*, 359−367.
(2) Kerr, J. B. Polymeric Electrolytes: An Overview. In *Lithium Batteries. Sience and Technology*; Nazri, G.-A., Pistoia, Eds.; Kluwer Academic Publishers: Boston, 2004.
(3) Kerr, J. B.; Sloop, S. E.; Liu, G.; Han, Y. B.; Hou, J.; Wang, S. *J. Power Sources* **2002**, *110*, 389−400.
(4) Trapa, P. E.; Acar, M. H.; Sadoway, D. R.; Mayes, A. M. *J. Electrochem. Soc.* **2005**, *152*, A2281−A2284.
(5) Allcock, H. R.; Welna, D. T.; Maher, A. E. *Solid State Ionics* **2006**, *177*, 741−747.
(6) Sun, X. G.; Hou, J.; Kerr, J. B. *Electrochim. Acta* **2005**, *50*, 1139−1147.
(7) Sun, X. G.; Reeder, C. L.; Kerr, J. B. *Macromolecules* **2004**, *37*, 2219−2227.
(8) Zhang, S. H.; Dou, S. C.; Colby, R. H.; Runt, J. *J. Non-Cryst. Solids* **2005**, *351*, 2825−2830.
(9) Munch Elmer, A.; Jannasch, P. *Solid State Ionics* **2006**, *177*, 573−579.
(10) Kaskhedikar, N.; Paulsdorf, J.; Burjanadze, M.; Karatas, Y.; Wilmer, D.; Roling, B.; Wiemhofer, H. D. *Solid State Ionics* **2006**, *177*, 703−707.
(11) Luther, T. A.; Stewart, F. F.; Budzien, J. L.; LaViolette, R. A.; Bauer, W. F.; Harrup, M. K.; Allen, C. W.; Elayan, A. *J. Phys. Chem. B* **2003**, *107*, 3168−3176.
(12) Allcock, H. R.; Napierala, M. E.; Olmeijer, D. L.; Best, S. A.; Merz, K. M. *Macromolecules* **1999**, *32*, 732−741.
(13) Allcock, H. R.; Napierala, M. E.; Olmeijer, D. L.; Cameron, C. G.; Kuharcik, S. E.; Reed, C. S.; O'Connor, S. J. M. *Electrochim. Acta* **1998**, *43*, 1145−1150.

(14) Buriez, O.; Han, Y. B.; Hou, J.; Kerr, J. B.; Qiao, J.; Sloop, S. E.; Tian, M. M.; Wang, S. G. *J. Power Sources* **2000**, *89*, 149−155.
(15) Watanabe, M.; Hirakimoto, T.; Mutoh, S.; Nishimoto, A. *Solid State Ionics* **2002**, *148*, 399−404.
(16) Matoba, Y.; Ikeda, Y.; Kohjiya, S. *Solid State Ionics* **2002**, *147*, 403−409.
(17) Jannasch, P. *Macromolecules* **2000**, *33*, 8604−8610.
(18) Seki, S.; Tabata, S.; Matsui, S.; Watanabe, M. *Electrochim. Acta* **2004**, *50*, 379−383.
(19) Watanabe, M.; Endo, T.; Nishimoto, A.; Miura, K.; Yanagida, M. *J. Power Sources* **1999**, *82*, 786−789.
(20) Muller-Plathe, F.; van Gunsteren, W. F. *J. Chem. Phys.* **1995**, *103*, 4745−4756.
(21) Smith, G. D.; Borodin, O.; Pekny, M.; Annis, B.; Londono, D.; Jaffe, R. L. *Spectrochim. Acta, Part A* **1997**, *53*, 1273−1283.
(22) Borodin, O.; Smith, G. D. *Macromolecules* **1998**, *31*, 8396−8406.
(23) Borodin, O.; Smith, G. D. *Macromolecules* **2000**, *33*, 2273−2283.
(24) Sawa, F.; Takimoto, J. I.; Aoyagi, T.; Fukunaga, H.; Shoji, T.; Doi, M. *Prog. Theor. Phys. Suppl.* **2000**, 408−409.
(25) Hyun, J. K.; Dong, H. T.; Rhodes, C. P.; Frech, R.; Wheeler, R. A. *J. Phys. Chem. B* **2001**, *105*, 3329−3337.
(26) Triolo, A.; Arrighi, V.; Triolo, R.; Passerini, S.; Mastragostino, M.; Lechner, R. E.; Ferguson, R.; Borodin, O.; Smith, G. D. *Physica B* **2001**, *301*, 163−167.
(27) van Zon, A.; de Leeuw, S. W. *Electrochim. Acta* **2001**, *46*, 1539−1544.
(28) Ferreira, B. A.; Muller-Plathe, F.; Bernardes, A. T.; De, Almeida, W. B. *Solid State Ionics* **2002**, *147*, 361−366.
(29) Kuppa, V.; Manias, E. *Chem. Mater.* **2002**, *14*, 2171−2175.
(30) Borodin, O.; Smith, G. D.; Bandyopadhyaya, R.; Redfern, P.; Curtiss, L. A. *Model. Simul. Mater. Sci. Eng.* **2004**, *12*, S73−S89.
(31) Siqueira, L. J. A.; Ribeiro, M. C. C. *J. Chem. Phys.* **2005**, *122*, 194911.
(32) Duan, Y. H.; Halley, J. W.; Curtiss, L.; Redfern, P. *J. Chem. Phys.* **2005**, *122*, -.
(33) Borodin, O.; Smith, G. D.; Geiculescu, O.; Creager, S. E.; Hallac, B.; DesMarteau, D. *J. Phys. Chem. B* **2006**, *110*, 24266−24274.
(34) Siqueira, L. J. A.; Ribeiro, M. C. C. *J. Chem. Phys.* **2006**, *125*, 214903−8.
(35) Annis, B. K.; Borodin, O.; Smith, G. D.; Benmore, C. J.; Soper, A. K.; Londono, J. D. *J. Chem. Phys.* **2001**, *115*, 10998−11003.
(36) Borodin, O.; Smith, G. D. *Macromolecules* **2006**, *39*, 1620−1629.
(37) Balbuena, P. B.; Lamas, E. J.; Wang, Y. X. *Electrochim. Acta* **2005**, *50*, 3788−3795.
(38) Wang, Y. X.; Balbuena, P. B. *J. Phys. Chem. B* **2004**, *108*, 15694−15702.
(39) Karo, J.; Aabloo, A.; Thomas, J. O. *Solid State Ionics* **2005**, *176*, 3041−3044.
(40) Borodin, O.; Smith, G. D. *J. Phys. Chem. B* **2006**, *110*, 6279−6292.
(41) Borodin, O.; Smith, G. D. *J. Phys. Chem. B* **2006**, *110*, 6293−6299.
(42) Ayyagari, C.; Bedrov, D.; Borodin, O.; Smith, G. D. Lucretius, MD simulation code http://lucretius.mse.utah.edu/.
(43) Frenkel, D.; Smit, B. *Understanding Molecular Simulation: From Algorithms to Applications*, 2nd ed.; Academic Press: New York, 2002.
(44) Martyna, G. J.; Tuckerman, M.; Tobias, D. J.; Klein, M. L. *Mol. Phys.* **1996**, *87*, 1117−1157.
(45) Henderson, W. A.; McKenna, F.; Khan, M. A.; Brooks, N. R.; Young, V. G.; Frech, R. *J. Phys. Chem. B* **2005**, *17*, 2284−2289.
(46) Borodin, O.; Smith, G. D. *Macromolecules* **1998**, *31*, 8396−8406.
(47) Borodin, O.; Smith, G. D.; Douglas, R. *J. Phys. Chem. B* **2003**, *107*, 6824−6837.
(48) Borodin, O.; Smith, G. D.; Jaffe, R. L. *J. Comput. Chem.* **2001**, *22*, 641−654.
(49) Xu, K. *Chem. Rev.* **2004**, *104*, 4303−4417.
(50) Borodin, O.; Smith, G. D.; Henderson, W. *J. Phys. Chem. B* **2006**, *110*, 16879−16886.
(51) Nishimoto, A.; Agehara, K.; Furuya, N.; Watanabe, T.; Watanabe, M. *Macromolecules* **1999**, *32*, 1541−1548.
(52) Mondello, M.; Grest, G. S. *J. Chem. Phys.* **1997**, *106*, 9327−9336.
(53) Hayamizu, K.; Akiba, E.; Bando, T.; Aihara, Y. *J. Chem. Phys.* **2002**, *117*, 5929−5939.
(54) Borodin, O.; Smith, G. D. *J. Phys. Chem. B* **2006**, *110*, 4971−4977.
(55) Zhang, Z. C.; Lyons, L. J.; Amine, K.; West, R. *Macromolecules* **2005**, *38*, 5714−5720.
(56) Zhang, Z. C.; Sherlock, D.; West, R.; West, R.; Amine, K.; Lyons, L. J. *Macromolecules* **2003**, *36*, 9176−9180.
(57) Hayamizu, K.; Aihara, Y.; Price, W. S. *J. Chem. Phys.* **2000**, *113*, 4785−4793.

MA062128S